Brain Struct Funct (2013) 218:105–121
DOI 10.1007/s00429-012-0386-5

ORIGINAL ARTICLE

Analysis of the subcomponents and cortical terminations of the perisylvian superior longitudinal fasciculus: a fiber dissection and DTI tractography study

Juan Martino · Philip C. De Witt Hamer · Mitchel S. Berger · Michael T. Lawton · Christine M. Arnold · Enrique Marco de Lucas · Hugues Duffau

Received: 6 August 2011 / Accepted: 18 January 2012 / Published online: 16 March 2012

Abstract The anatomy of the perisylvian component of the superior longitudinal fasciculus (SLF) has recently been reviewed by numerous diffusion tensor imaging tractography (DTI) studies. However, little is known about the exact cortical terminations of this tract. The aim of the present work is to isolate the different subcomponents of this tract with fiber dissection and DTI tractography, and to identify the exact cortical connections. Twelve postmortem human hemispheres (6 right and 6 left) were dissected using the cortex-sparing fiber dissection. In addition, three healthy brains were analyzed using DTI-based tractography software. The different components of the perisylvian SLF were isolated and the fibers were followed until the cortical terminations. Three segments of the perisylvian SLF were identified: (1) anterior segment, connecting the supramarginal gyrus and superior temporal gyrus with the precentral gyrus, (2) posterior segment, connecting the posterior portion of the middle temporal gyrus with the angular gyrus, and (3) long segment of the arcuate fasciculus that connects the middle and inferior temporal gyri with the precentral gyrus and posterior portion of the inferior and middle frontal gyri. In the present study, three different components of the perisylvian SLF were identified. For the first time, our dissections revealed that each component was connected to a specific cortical area within the frontal, parietal and temporal lobes. By accurately depicting not only the trajectory but also cortical connections of this bundle, it is possible to develop new insights into the putative functional role of this tract.

Keywords Arcuate fasciculus · DTI tractography · Fiber dissection · Superior longitudinal fasciculus

Abbreviations

AF	Arcuate fasciculus
AG	Angular gyrus
DTI	Diffusion tensor imaging
IES	Intraoperative electrical stimulation
IFG	Inferior frontal gyrus
ITG	Inferior temporal gyrus
MFG	Middle frontal gyrus
PCG	Precentral gyrus
SF	Sylvian fissure

J. Martino (✉)
Department of Neurological Surgery, Hospital Universitario Marqués de Valdecilla and Instituto de Formación e Investigación Marqués de Valdecilla (IFIMAV), Av de Valdecilla s/n, 39008 Santander, Cantabria, Spain
e-mail: juan.martino@hotmail.com

P. C. De Witt Hamer
Department of Neurological Surgery, VU University Medical Center, Amsterdam, The Netherlands

M. S. Berger · M. T. Lawton · C. M. Arnold
Department of Neurological Surgery, University of California San Francisco (UCSF), San Francisco, CA, USA

E. M. de Lucas
Department of Radiology, Hospital Universitario Marqués de Valdecilla and Instituto de Formación e Investigación Marqués de Valdecilla (IFIMAV), Av de Valdecilla s/n, Santander, Cantabria, Spain

H. Duffau
Department of Neurological Surgery, Hôpital Gui de Chauliac, CHU Montpellier, 80 Av Augustin Fliche, 34295 Montpellier, France

H. Duffau
INSERM U1051, Institute for Neurosciences of Montpellier, Hôpital Saint Eloi, CHU Montpellier, 80 Av Augustin Fliche, 34295 Montpellier, France

SLF	Superior longitudinal fasciculus
SMG	Supramarginal gyrus
SPL	Superior parietal lobe
STG	Superior temporal gyrus

Introduction

The superior longitudinal fasciculus (SLF) was first described by Reil and Autenrieth at the beginning of the nineteenth century as a group of fibers located into the white matter of the temporal, parietal and frontal regions, and around the Sylvian fissure. Burdach (1819–1826) and subsequently Dejerine (1895), following this initial identification of the tract, described in detail this fiber system as a tract that arches around the Sylvian fissure and connects the posterior temporal lobe with the frontal lobe. They named this bundle the *Fasciculus Arcuatus* and considered it as part of the SLF, using interchangeably the terms "superior longitudinal fasciculus" or "fasciculus arcuatus" in their descriptions.

Magnetic resonance imaging may be sensitized to diffusion of water molecules in the direction of the field gradient. Diffusion tensor is a mathematic model of diffusion of water molecules in 3D space. The tensor is a matrix of numbers derived from diffusion measurements in several different directions, from which one can estimate the diffusivity in any arbitrary direction or determine the direction of maximum diffusivity. Within white matter, diffusion is anisotropic (directionally dependent) as axonal membranes and myelin sheaths present barriers to the motion of water molecules in directions not parallel to their own orientation (Jellison et al. 2004). Based on these principles, diffusion tensor imaging (DTI) tractography is able to map white matter fiber direction, providing a unique opportunity to study white matter architecture in vivo (Catani et al. 2002, 2003, 2005; Le et al. 2001; Mori and van Zijl 2002; Hagmann et al. 2003). Recent neuroimaging studies based on DTI tractography have revealed that the SLF is a complex brain association fiber system composed of two parallel pathways connecting temporal, parietal and frontal regions (Fig. 1) (Catani et al. 2005; Catani and de Thiebaut 2008; Fernandez-Miranda et al. 2008b; Lawes et al. 2008; Gharabaghi et al. 2009): (1) a direct pathway corresponding to the classical AF; (2) an indirect pathway, running parallel and lateral to the direct pathway, and consisting of an anterior segment linking the lateral frontal cortex with the inferior parietal lobe, and a posterior segment linking the inferior parietal lobe with the temporal lobe. Isotope studies in non-human primates (Petrides and Pandya 1984; Schmahmann and Pandya 2006; Schmahmann et al. 2007) as well as DTI analyses in humans (Makris et al. 2005) had identified two additional non-perisylvian components of the SLF. These tracts are named the SLF I and II, and are horizontal fronto-parietal connections that run within the white matter of the parietal and frontal lobes.

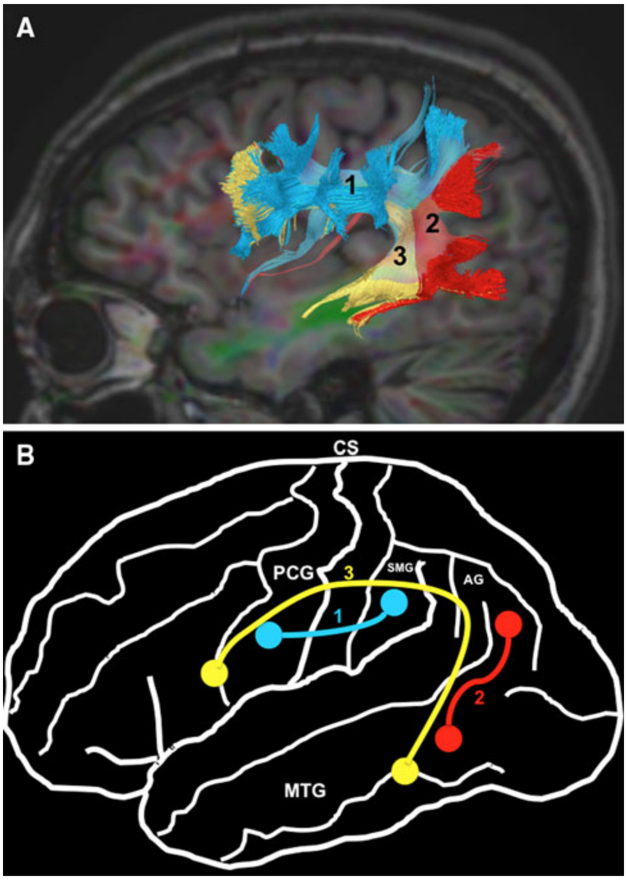

Fig. 1 **a** DTI tractography reconstruction of the perisylvian component of the superior longitudinal fasciculus (SLF). **b** Schematic representation of the perisylvian component of the SLF. *1* anterior segment of the SLF; *2* posterior segment of the SLF; *3* arcuate fasciculus. *AG* angular gyrus; *CS* central sulcus; *PCG* precentral gyrus; *MTG* middle temporal gyrus; *SMG* supramarginal gyrus; *STG* superior temporal gyrus

Consequently, DTI methodology applied to the human brain has been very useful in providing visualization of the core of pathways that compose the SLF. However, average anisotropy in voxels does not allow tracking single terminal branches of the white matter bundles, so that their final cortical destination can only be indirectly inferred from the location and orientation of the average tract end points (Catani et al. 2003; Petrides and Pandya 2009). This probably explains the confusing and contradicting DTI reports of the cortical connections of the SLF (Catani and de Thiebaut 2008; Fernandez-Miranda et al. 2008b; Lawes et al. 2008; Gharabaghi et al. 2009; Makris et al. 2005; Rilling et al. 2008; Bernal and Ardila 2009; Barrick et al. 2007; Henry et al. 2004; Catani et al. 2005).

Autoradiography tract tracing is generally considered the anatomical gold standard to validate DTI findings; however, these studies are of course impossible in humans (Schmahmann et al. 2007, 2004; Giolli et al. 2001). Alternatively, the technique of fiber dissection in postmortem human brains, first described by Klingler (1935); Ludwig and Klingler (1956); Klingler and Gloor (1960), and based on freezing of the brains during the fixation process—with spreading of this freezing along the white matter fibers—can provide isolation and tracking of terminal fiber bundles in postmortem human brain. However, classical fiber dissection requires removal of the cortex and overlying white matter in order to reveal the deeper tracts (Peuskens et al. 2004; Klingler 1935; Klingler and Gloor 1960; Choi et al. 2006; Sincoff et al. 2004; Ture et al. 1997, 1999, 2000; Lawes et al. 2008; Glasser and Rilling 2008; Fernandez-Miranda et al. 2008a, b; Ludwig and Klingler 1956). Our group initially performed classical fiber dissection, but then we realized that the extensive removal of surrounding brain tissue precludes the orientation of tracts in relation to cortical landmarks which hampers analysis of cortical terminations. Therefore, we developed a modification of the classical fiber dissection methodology in which removal of brain tissue was kept to a minimum to preserve the cortex and relationships within the brain until the end of dissection. Consequently, the trajectory and the orientation of white matter tracts can now be identified reliably and reproducibly. We postulate this dissection technique as "cortex-sparing fiber dissection" referring to the fact that the cortex is preserved until the end of the dissection (Martino et al. 2010a, b, 2011).

Numerous publications have previously demonstrated that the in vivo reconstructions of DTI tractography are very close to the postmortem findings derived from fiber dissections (Catani et al. 2002; Catani and de Thiebaut 2008; Fernandez-Miranda et al. 2008a, b; Kier et al. 2004a, b; Thiebaut de Schotten et al. 2011). Our group recently isolated the three components of the perisylvian SLF using fiber dissection and DTI tractography (Martino et al. 2011). In the present work, both techniques were used to identify the exact cortical connections of this tract, i.e., the cortical areas where the axons of the three subcomponents of this tract terminate. The accurate depicting of the connectional architecture of this important bundle is essential to understand the functional role of these connections within the language network.

Materials and methods

Cortex-sparing fiber dissection

Twelve human cerebral hemispheres (6 right side and 6 left side) were removed from bodies embalmed with 10% formalin solution for at least 40 days. The mean age of the subjects from whom brains were obtained was 69 years (range 60–75 years). The piamater, arachnoid membrane and vascular structures were carefully removed and the hemispheres were frozen at −15°C for 15 days. The water crystallization induced by the freezing process disrupts the structure of the gray matter (with high water content), enabling the peeling off the cortex from the brain surface. The freezing process also spreads along the white matter fibers, facilitating the dissection of the fiber tracts.

Before the dissection started, a detailed study of the surface anatomy of the sulci and gyri was made. The specimens were dissected in a stepwise manner, from lateral to medial. With classical fiber dissection, the demonstration of one fiber system results in the destruction of other fiber systems (Klingler 1935; Ludwig and Klingler 1956; Klingler and Gloor 1960; Ture et al. 2000). The removal of overlying brain structures, however, prohibits the correlation of white matter tracts with cortical terminations. In the present study, overlying brain structures were preserved along the dissection to analyze the anatomical cortical connectivity of the SLF. The dissection methodology presented in this study has been previously described by our group (Martino et al. 2010a, b, 2011).

The first step is to remove the cortex within the depth of the sulci only, with preservation of the cortex of the convexity surface of the gyri (Fig. 2). This is a crucial step in the dissection, as it provides space to dissect the white matter but at the same time preserves the cortical anatomical landmarks until the end of the dissection. Then, the stem of superior, middle and inferior temporal gyri were cut in a plane perpendicular to the convexity surface of the hemisphere, and the anatomic planes of cleavage between the fibers were opened enabling the following of the fibers of the SLF (Figs. 2, 3, 4). Care was taken to avoid transecting axons, by utilizing blunt rather than sharp dissection, thus minimizing the risk of spurious tracts. With careful dissection, it was possible to completely isolate the fibers of the SLF from the other bundle and to follow the fibers of the tract until they enter the gray matter at the cortex (Figs. 3, 4). The Atlas of the Cerebral Sulci of Ono et al. (1990) was used to validate the specific cortical connections identified.

The dissections were performed under loupes magnification (3.2×), enabling the isolation of fibers up to 2 mm in diameter. Consequently, it was not possible to follow smaller branches of the SLF. Handmade wooden spatulas were used in the initial steps of the dissection to remove the brain cortex within the depth of the sulci. Once the fibers of the SLF were identified, the remaining dissection was performed using curving metallic dissectors with various tip sizes. Sequential digital pictures were taken during the dissection.

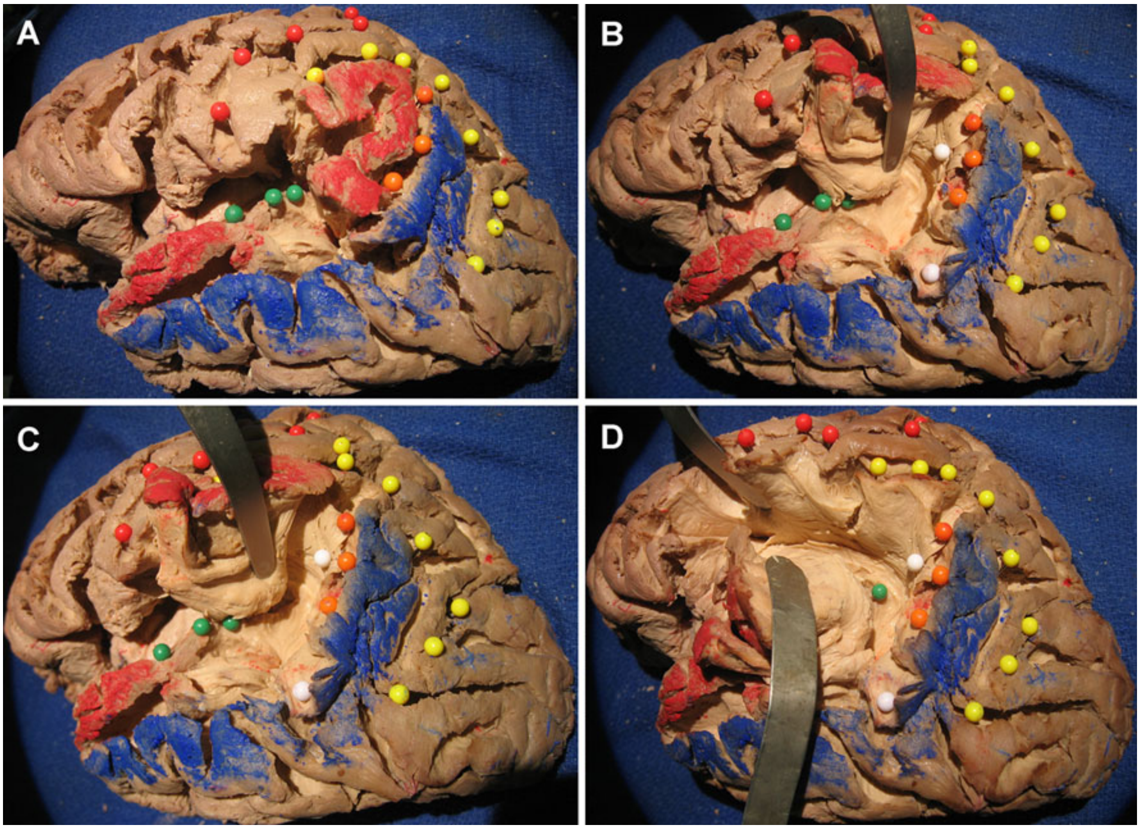

Fig. 2 Stepwise fiber dissection of the anterior segment of the perisylvian component of the superior longitudinal fasciculus (SLF) in a left hemisphere. **a** Lateral surface of the hemisphere following the removal of the pia mater, arachnoid membranes and the cortex within the depth of the sulci. The cortex of the convexity surface of the gyri was not removed in order to preserve the anatomical landmarks until the end of the dissection. The superior temporal gyrus and the supramarginal gyrus are marked in *red*; the middle temporal gyrus and the angular gyrus are marked in *blue*. *Red spheres* mark the central sulcus, *yellow spheres* mark the intraparietal sulcus, *orange spheres* mark the intermediate sulcus of Jensen and *green spheres* mark the Heschl's gyrus. The *white arrow* defines the boundary between the superior temporal gyrus and the supramarginal gyrus at the angle between the terminal ascending ramus of the sylvian fissure and the posterior ramus of the sylvian fissure. The dissection started at the posterior portion of the superior temporal gyrus, just behind the Heschl's gyrus. At this level, the fibers of the anterior segment of the SLF were easily separated from the auditory radiations that originate at the primary auditory area in the Heschl's gyrus. This tract is caudally connected to the supramarginal gyrus and the posterior portion of the superior temporal gyrus. **b**, **c** and **d** Stepwise dissection of the tract, separating it from the surrounding fiber tracts. The fibers of this bundle have a superior and posterior orientation, then they curve around the caudal end of the Sylvian fissure to take an anterior orientation, and run within the *white* matter of the parietal and frontal operculum and terminate at the precentral gyrus

Diffusion tensor imaging tractography analysis

Three healthy volunteers of 23, 30 and 31 years old were studied with brain MRI performed on a whole-body 3.0-T scanner (Achieva 3.0T; Philips Healthcare, Best, The Netherlands) with an eight-channel head coil. DTI was performed using a single-shot multislice spin echo–echo planar sequence with the following attributes: diffusion sensitization, 1,300 s/mm^2; TR, 9,577 ms; TE, 77 ms; voxel size 2 mm; no gap between slices; matrix, 224 × 224. Sixty-four diffusion gradient directions were obtained. The DTI data sets and anatomic MRI scans were analyzed with Fiber Trak software for diffusion tensor analysis and fiber tracking from MR Workspace (Philips Healthcare).

We applied a knowledge-based multiple region-of-interest approach (ROI) in which the tracking algorithm was initiated from user-defined seed regions. Axonal projections were traced both in anterograde and retrograde directions according to the direction of the principal eigenvector in each voxel of the region of interest. Tracking terminated when the fractional anisotropy value was lower than 0.18. The cortical connections of the tracts were inferred from the location and orientation of the average tract end points (Catani et al. 2003; Petrides and Pandya 2009).

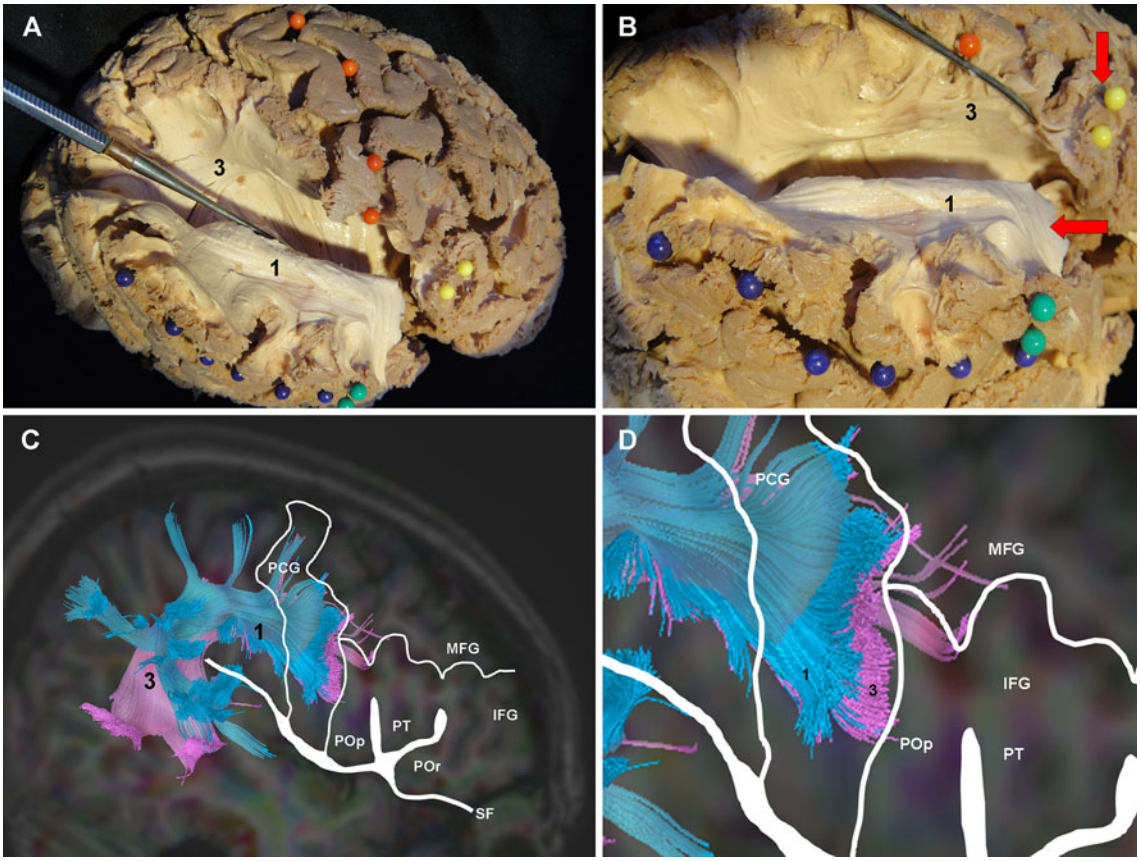

Fig. 3 **a** Fiber dissection of the anterior portion of the superior longitudinal fasciculus (SLF) (*1*) and arcuate fasciculus (AF) (*2*) in a right hemisphere. *Blue spheres* mark the sylvian fissure, *red spheres* mark the superior portion of the central sulcus, *green spheres* mark the inferior portion of the central sulcus, and *yellow spheres* mark the pars opercular of the inferior fontal gyrus. The frontal and parietal operculum with the anterior portion of the SLF was tilted inferiorly, while the fibers of the arcuate fasciculus were located superiorly. The precentral gyrus is divided into two; the anterior portion of the SLF is connected to the ventral portion of the precentral gyrus, while the AF is connected to the dorsal portion. **b** Detailed view of the termination of the anterior portion of the SLF at the precentral gyrus (marked by the *horizontal red arrow*), and the termination of the AF at the pars opercularis of the inferior frontal gyrus (marked by the *vertical red arrow* and the *yellow spheres*). **c** DTI tractography reconstruction of the anterior segment of the SLF (*1*) and the AF (*3*). **d** Detailed view of the termination of the anterior portion of the SLF at the precentral gyrus, and the termination of the AF at the precentral gyrus and posterior portion of the middle frontal gyrus. *IFG* inferior frontal gyrus; *MFG* middle frontal gyrus; *PCG* precentral gyrus; *POp* pars opercularis of the inferior frontal gyrus; *POr* pars orbicularis of the inferior frontal gyrus; *PT* pars triangularis of the inferior frontal gyrus

Statistical analysis

Frequency distributions and summary statistics were calculated for all variables; values are expressed as mean and range. A Kolmogorov–Smirnov test was used to study the distribution of each variable and P–P and Q–Q charts were used to confirm it. The majority did not follow a normal distribution, and non-parametric tests were used for comparisons. A Mann–Whitney *U* test was used to determine the relationship between the independent variable (right vs. left hemispheres) and quantitative variables (two distances measured at the AF). A Fisher′s exact test was used to determine the relationship between the independent variable (right vs. left hemispheres) and qualitative variables (identification of each subcomponent of the tract). A significance level of 5% ($p < 0.05$) was accepted in all cases. SPSS software version 18.0 (SPSS, UK) was used for the statistical analysis.

Results

A detailed analysis of the surface anatomy of each hemisphere was performed, and variations in the gyral and sulcal pattern were noted. The present dissection and DTI tractography analysis revealed that the perisylvian SLF can be clearly divided into three different components: two superficial short tracts and one long deep tract or AF. The cortical connections of the three segments of the SLF and the distances measured at the AF in each hemisphere are listed in Tables 1 and 2.

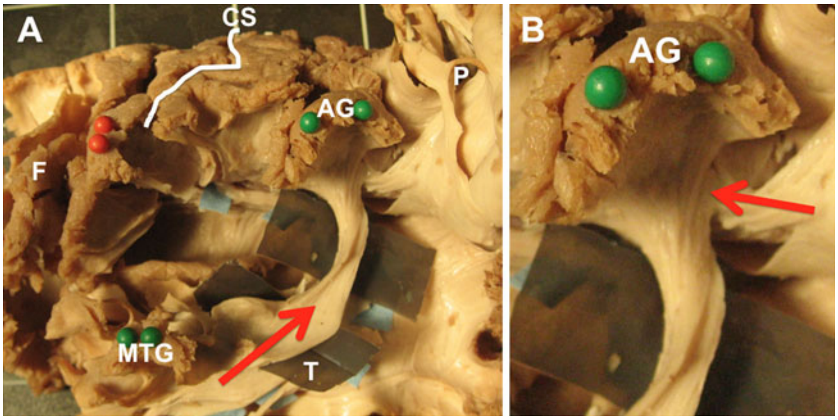

Fig. 4 **a** Fiber dissection of the posterior segment of the perisylvian superior longitudinal fasciculus (SLF) (*red arrow*) in a left hemisphere. This tract is composed of a well-defined group of vertically oriented fibers that run laterally to the arcuate fasciculus (AF) and connect the posterior portion of the middle temporal gyrus with the angular gyrus. Small pieces of *black* paper were placed between the posterior portion of the SLF and the AF. **b** Detailed view of the terminal fibers of the posterior portion of the SLF (*arrow*) connected to the AG. *AG* angular gyrus; *CS* central sulcus; *F* fontal lobe; *MTG* middle temporal gyrus; *P* superior parietal lobe; *T* temporal lobe

Anterior segment of the perisylvian component of the SLF

This connection was identified in 11 out of the 12 hemispheres (91.7%) dissected. The dissection started at the posterior portion of the superior temporal gyrus, just behind the Heschl's gyrus. At this level, the fibers of the SLF were easily separated from the auditory radiations that originated at the primary auditory area in the Heschl's gyrus (Rhoton 2002). The fibers of this portion of the SLF had a superior and posterior orientation; then they curved around the caudal end of the Sylvian fissure to take an anterior orientation and ran within the white matter of the parietal and frontal operculum lateral to the AF. Finally, they terminated at the posterior portion of the frontal operculum (Figs. 2, 3). Regarding the posterior cortical termination of this bundle, in nine hemispheres (82%) it was connected to the supramarginal gyrus and the posterior portion of the superior temporal gyrus. In one hemisphere, it was also connected to the angular gyrus. At the level of the frontal operculum, in eight hemispheres (73%), the fibers of this bundle were connected to the ventral portion of the precentral gyrus (Figs. 3, 8). In three hemispheres, the bundle was connected to the frontal operculum but, due to the strong intersection with other fibers, it was not possible to follow the exact frontal cortical termination of the tract.

This connection was identified in all the hemispheres studied with DTI tractography. Regarding the posterior cortical termination of this bundle, in all the hemispheres it was connected to the supramarginal gyrus. In three hemispheres (50%), it was also connected to the posterior portion of the superior temporal gyrus. In two hemispheres (33%), it was also connected to the angular gyrus. At the level of the frontal operculum, in all the hemispheres the tract was connected to the ventral portion of the precentral gyrus (Figs. 3, 8). In two hemispheres (33%), it was also connected to the posterior portion of the inferior frontal gyrus.

Posterior segment of the perisylvian component of the SLF

This connection was identified in 8 out of 12 hemispheres (67%) dissected. The dissection started at the posterior portion of the middle temporal gyrus. The dissection revealed a well-defined group of vertically oriented fibers that ran lateral to the AF and terminated at the inferior parietal lobe (Figs. 4, 8). Regarding the inferior cortical termination of this bundle, in all the hemispheres this tract was connected to the posterior portion of the middle temporal gyrus. Superiorly, it was connected to the angular gyrus in seven hemispheres (88%), and in one hemisphere was also connected to the supramarginal gyrus and inferior portion of the superior parietal lobe.

This connection was identified in five out of six hemispheres (83%) studied with DTI tractography (Fig. 5). Regarding the inferior cortical termination, in four hemispheres (80%) it was connected to the posterior portion of the middle temporal gyrus, in two hemispheres (40%) to the inferior temporal gyrus and in one hemisphere (20%) to the superior temporal gyrus. Superiorly, this bundle was connected to the angular gyrus in four out of five hemispheres (80%), and in three hemispheres (60%) was connected to the supramarginal gyrus (Fig. 8).

Long segment of the perisylvian SLF

This connection was identified in all the hemispheres dissected. This long segment corresponds to the classical AF

Table 1 Cortical connections of the three segments of the perisylvian SLF obtained by fiber dissection

No.	Side	Anterior segment		Posterior segment		Arcuate fasciculus			
		Posterior connection	Anterior connection	Inferior connection	Superior connection	Posterior connection	Anterior connection	D1 (mm)	D2 (mm)
1	R	SMG, STG (POST)	PCG (VENT)	NO	NO	ITG (POST), MTG (MID)	PCG (VENT), IFG (POST)	16	27
2	L	SMG, STG (POST)	PCG (VENT)	MTG (POST)	AG	ITG (POST), MTG (MID)	PCG (VENT), IFG (POST), MFG (POST)	18	28
3	R	SMG, STG (POST)	PCG (VENT)	MTG (POST)	AG	ITG (POST), MTG (MID)	PCG (VENT), IFG (POST), MFG (POST)	24	28
4	L	NO	NO	MTG (POST)	AG, SMG, SPL	ITG (POST), MTG (MID)	PCG (VENT), IFG (POST), MFG (POST)	12	22
5	R	SMG, STG (POST)	PCG (VENT)	NO	NO	ITG (POST), MTG (MID)	PCG (VENT), IFG (POST), MFG (POST)	20	32
6	L	SMG, STG (POST)	PCG (VENT)	MTG (POST)	AG	ITG (POST), MTG (MID)	PCG (VENT), IFG (POST), MFG (POST)	18	32
7	R	SMG, STG (POST), AG	PCG (VENT)	NO	NO	ITG (POST), MTG (MID)	PCG (VENT), IFG (POST), MFG (POST)	25	40
8	L	SMG, STG (POST)	NP	MTG (POST)	AG	ITG (POST), MTG (MID)	NP	22	32
9	R	SMG, STG (POST)	NP	MTG (POST)	AG	ITG (POST), MTG (MID)	NP	20	30
10	L	SMG, STG (POST), AG	PCG (VENT)	NO	NO	ITG	PCG (VENT), IFG (POST)	20	30
11	R	SMG, STG (POST)	PCG (VENT)	MTG (POST)	AG	ITG	PCG (VENT), IFG (POST), MFG (POST)	19	32
12	L	SMG, STG (POST)	NP	MTG (POST)	AG	ITG (POST), MTG (POST)	NP	20	35
Total		SMG 100% STG 100% AG 18%	PCG 72%	MTG 100%	AG 100% SMG 13% SPL 13%	ITG 100% MTG 83%	PCG 75% IFG 75% MFG 58%	Mean 19 mm (12–25 mm)	Mean 30 mm (22–40 mm)

D1: antero-posterior distance between the most anterior point where the Heschl's gyrus intersects the inferior limiting sulcus of the insula and the posterior edge of the arcuate fasciculus (AF). D2: antero-posterior distance between the most posterior point where the Heschl's gyrus intersects the inferior limiting sulcus of the insula and the posterior edge of the AF

AG angular gyrus, *ANT* anterior, *IFG* inferior frontal gyrus, *ITG* inferior temporal gyrus, *MFG* middle frontal gyrus, *MID* middle, *MTG* middle temporal gyrus, *PCG* precentral gyrus, *NO* the tract was not identified in this hemisphere, *NP* not possible to identify the exact cortical termination, *PCG* precentral gyrus, *POST* posterior, *SMG* supramarginal gyrus, *STG* superior temporal gyrus, *VENT* ventral

Table 2 Cortical connections of the three segments of the perisylvian SLF obtained by diffusion tensor imaging (DTI) tractography

No	Side	Anterior segment		Posterior segment		Arcuate fasciculus			
		Posterior connection	Anterior connection	Inferior connection	Superior connection	Posterior connection	Anterior connection	D1 (mm)	D2 (mm)
1	R	SMG, STG (POST), AG	PCG (VENT), IFG (POST)	MTG (POST), ITG (POST)	AG	ITG (POST), MTG (POST)	PCG (VENT), MFG (POST)	12	23
2	L	SMG, STG (POST)	PCG (VENT)	ITG (POST)	AG	ITG (POST), MTG (POST)	PCG (VENT), IFG (POST)	11	18
3	R	SMG	PCG (VENT)	MTG (POST)	AG, SMG	NO	NO		
4	L	SMG	PCG (VENT)	NO	NO	MTG (MID)	PCG (VENT)	18	29
5	R	SMG, STG (POST), AG	PCG (VENT)	MTG (POST)	SMG, AG	MTG (POST)	IFG (POST)	13	26
6	L	SMG	PCG (VENT), IFG (POST)	MTG (POST), STG (POST)	SMG	MTG (POST)	PCG (VENT), IFG (POST)	12	17
Total		SMG 100% STG 50% AG 33%	PCG 100% IFG 33%	MTG 80% ITG 40% STG 20%	AG 80% SMG 60%	MTG 100% ITG 40%	PCG 80% IFG 60% MFG 20%	Mean 13 mm (11–18 mm)	Mean 23 mm (17–29 mm)

D1: antero-posterior distance between the most anterior point where the Heschl's gyrus intersects the inferior limiting sulcus of the insula and the posterior edge of the arcuate fasciculus (AF). D2: antero-posterior distance between the most posterior point where the Heschl's gyrus intersects the inferior limiting sulcus of the insula and the posterior edge of the AF

AG angular gyrus, *ANT* anterior, *IFG* inferior frontal gyrus, *ITG* inferior temporal gyrus, *MFG* middle frontal gyrus, *MID* middle, *MTG* middle temporal gyrus, *NO* the tract was not identified in this hemisphere, *PCG* precentral gyrus, *POST* posterior, *SMG* supramarginal gyrus, *STG* superior temporal gyrus, *VENT* ventral

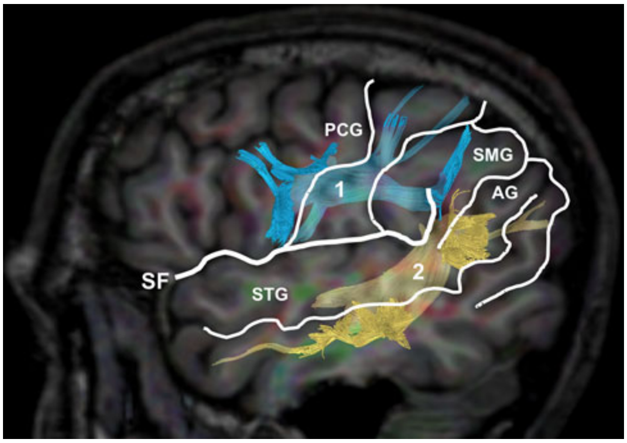

Fig. 5 DTI tractography reconstruction of the anterior segment of the SLF (*1*) and the posterior segment of the SLF (*2*). The anterior segment of the SLF is connected to the precentral gyrus and supramarginal gyrus. The posterior segment of the SLF is connected to the middle temporal gyrus and angular gyrus. *AG* angular gyrus; *PCG* precentral gyrus; *SF* sylvian fissure; *SMG* supramarginal gyrus; *STG* superior temporal gyrus

that is a long white matter tract deeply located to the parieto-frontal and temporo-parietal segments of the SLF (Figs. 6, 7). After lifting these two superficial connections, the lateral surface of the AF was completely exposed. At this point, it is important to remark that the dissection technique used here enabled us to isolate this deeper bundle without destroying the superficial components of the fascicle (Fig. 6). In the next step of the dissection, the deep surface of the bundle was carefully separated from the deeper structures. This dissection started by opening the stem of the inferior temporal gyrus. Then, the deep surface of the bundle was carefully separated from the deeper structures. A clear plane of cleavage was identified between the fibers of the AF that had a superior–inferior orientation at the temporal lobe and the fibers of the sagittal stratum (i.e., densely packed fibers located at the lateral surface of the atrium and composed of the optic radiations, inferior fronto-occipital fasciculus and tapetum) with an anterior–posterior orientation. This plane was carefully dissected, following the direction of the fibers that curved around the caudal limit of the insula to take a horizontal direction and anterior orientation and then ran within the white matter of the parietal and frontal operculum lateral to the cortico-spinal tract that had a vertical direction (Fig. 7). Finally they terminated at the posterior portion of the frontal operculum.

Regarding the posterior cortical termination of this bundle, in all the hemispheres this tract was connected to the inferior temporal gyrus, and in ten hemispheres (83%) to the middle temporal gyrus (Figs. 6, 8). At the level of the frontal operculum, in nine hemispheres (75%) it was connected to the ventral portion of the precentral gyrus (Figs. 6, 7, 8). In nine hemispheres (75%), it was connected to the posterior portion of the inferior frontal gyrus. In seven hemispheres (58%), it was connected to the middle frontal gyrus (Fig. 3). In three hemispheres, the bundle was

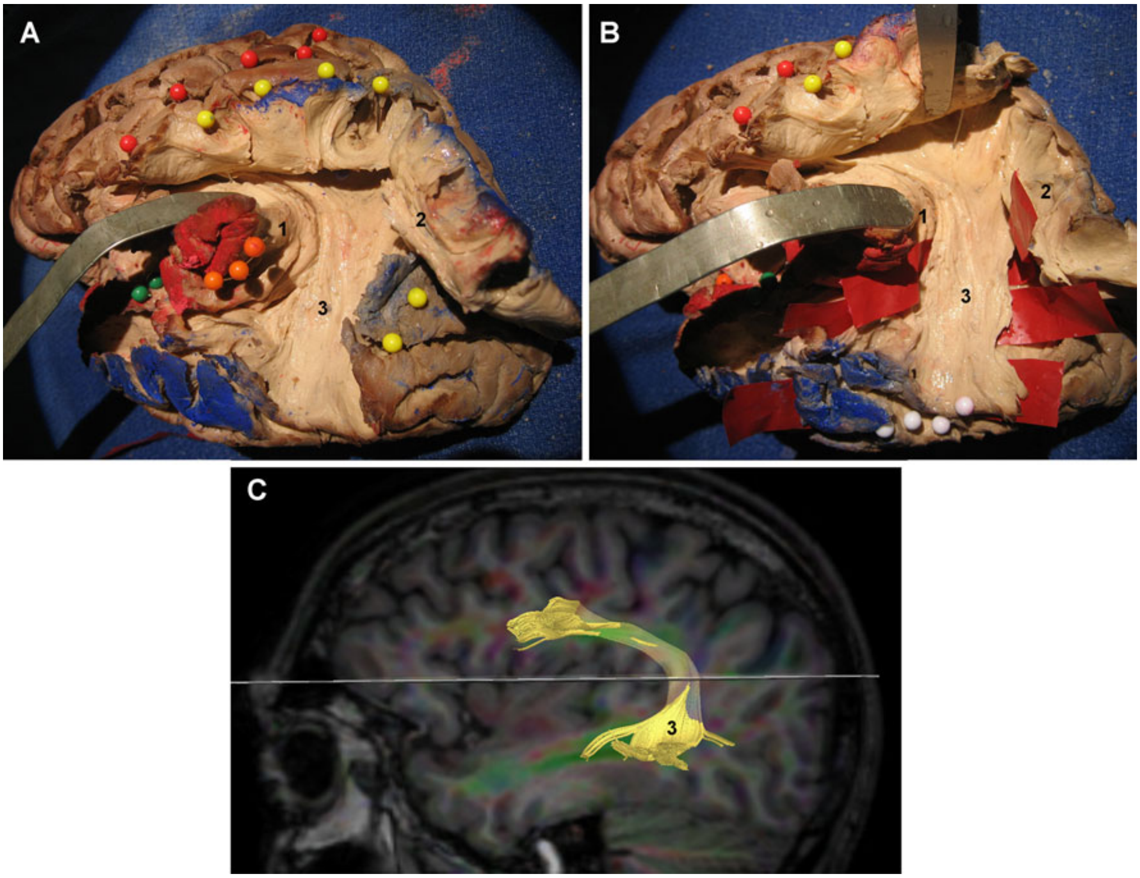

Fig. 6 Fiber dissection and DTI tractography reconstruction of the long segment of the superior longitudinal fasciculus (SLF) or arcuate fasciculus (AF) (*3*). **a** The superior temporal gyrus and the supramarginal gyrus are marked in *red*; the middle temporal gyrus and the angular gyrus are marked in *blue*. *Red spheres* mark the central sulcus, *yellow spheres* mark the intraparietal sulcus, *orange spheres* mark the intermediate sulcus of Jensen and *green spheres* mark the Heschl's gyrus. The posterior portion of the SLF was titled to expose the fibers of the AF. As evidenced in the picture, we were able to isolate this deeper bundle without destroying the superficial components of the fascicle. **b** Small pieces of *red* paper were placed between the AF and the fibers of the sagittal stratum (i.e., densely packed fibers located at the lateral surface of the atrium and composed of the optic radiations, IFOF and tapetum). It is evidenced that the AF is posteriorly connected to the inferior temporal gyrus (marked with *white spheres*) and to the middle portion of the middle temporal gyrus (marked in *blue*). **c** DTI tractography reconstruction of the AF. (*1*) anterior segment of the SLF; (*2*) posterior segment of the SLF; (*3*) arcuate fasciculus

connected to the frontal operculum, but due to the strong intersection with other fibers it was not possible to follow the exact frontal cortical termination of the tract.

This connection was identified in five out of six hemispheres (83%) studied with DTI tractography. Regarding the posterior cortical termination, in all the hemispheres it was connected to the middle temporal gyrus, and in two hemispheres (40%) also to the inferior temporal gyrus. At the level of the frontal operculum, in four hemispheres (80%) it was connected to the ventral portion of the precentral gyrus (Figs. 6, 8), in three hemispheres (60%) to the posterior portion of the inferior frontal gyrus (Fig. 3), and in one hemisphere (20%) to the posterior portion of the middle frontal gyrus.

It is important that connections of the AF to the superior temporal gyrus were not identified either in fiber dissection or in DTI tractography. As previously explained, the fibers from the superior temporal gyrus converged into the anterior portion of the SLF.

Two distances were measured at the AF (Fig. 7; Tables 1, 2). The two distances were measured in a line that passed through the inferior limiting sulcus of the insula. The first measurement is the distance between the most anterior point where the Heschl's gyrus intersects the inferior limiting sulcus of the insula and the posterior edge of the AF (fiber dissection: average 19 mm, range 12–25 mm; DTI tractography: average 13 mm, range 11–18 mm). The second measurement is the antero-posterior distance between the most posterior point where the Heschl's gyrus intersects the inferior limiting sulcus of the insula (this anatomic point corresponds to the most caudal point of the insula, at the junction of the inferior and superior limiting sulcus) and the posterior edge of the AF (fiber dissection: average 30 mm, range 22–40 mm; DTI

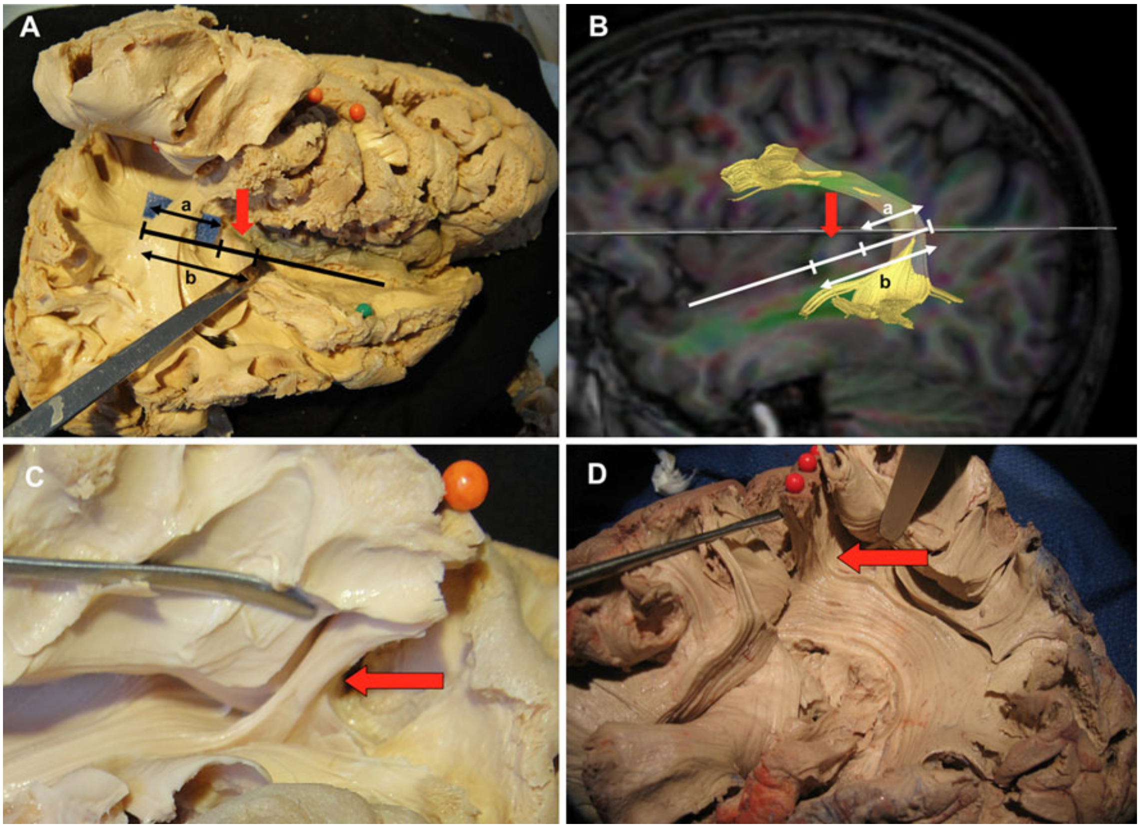

Fig. 7 Fiber dissection and DTI tractography reconstruction of the long segment of the superior longitudinal fasciculus (SLF) or arcuate fasciculus (AF). **a** and **b** Two distances were measured in a line that passes through the inferior limiting sulcus of the insula: distance-a is the antero-posterior distance between the most posterior point where the Heschl's gyrus (marked with a *vertical red arrow*) intersects the inferior limiting sulcus (this anatomic point corresponds to the most caudal point of the insula, at the junction of the inferior and superior limiting sulcus of the insula) and the posterior edge of the AF. Distance-b is the antero-posterior distance between the most anterior point where the Heschl's gyrus intersects the inferior limiting sulcus and the posterior edge of the AF. **c** Detailed view of the terminal fibers of the AF (arrow) connecting to the precentral gyrus. **d** The fibers of the AF curve around the caudal limit of the insula to take a horizontal direction and anterior orientation, then run within the *white* matter of the parietal and frontal operculum lateral to the cortico-spinal tract that has a vertical direction (marked with a *horizontal red arrow*). The precentral gyrus is marked with *red spheres*

tractography: average 23 mm, range 17–29 mm). The two distances were compared between the right and left sides, and the differences observed were not statistically significant ($p > 0.05$). The projection of the caudal end of the AF in the convexity surface of the hemisphere is located at the posterior portion of the angular gyrus.

The identification of each tract and the cortical terminations were compared between the right and left sides; any of the differences observed were statistically significant ($p > 0.05$).

Discussion

The present work investigated the anatomical connectivity of the perisylvian component of the SLF by means of fiber dissection and DTI tractography. Comparable to previous DTI studies (Fernandez-Miranda et al. 2008b; Gharabaghi et al. 2009; Catani et al. 2005), we found three different components of this perisylvian tract: (1) a superficial anterior segment connecting the supramarginal gyrus and the superior temporal gyrus with the lateral frontal cortex, (2) a superficial posterior segment connecting the middle temporal gyrus with the angular gyrus, and (3) a deep and long tract connecting the middle and inferior temporal gyri with the lateral frontal cortex, representing the classical AF.

Anterior segment of the perisylvian component of the SLF

Catani et al. (2005) were the first to describe this connection in humans with DTI tractography. However, to our knowledge, there is only one previous paper that isolated this connection with fiber dissection. Fernandez-Miranda et al. (2008b) analyzed the three-dimensional anatomy of the SLF by means of fiber dissection and DTI tractography. Using fiber dissection, they were able to isolate the three

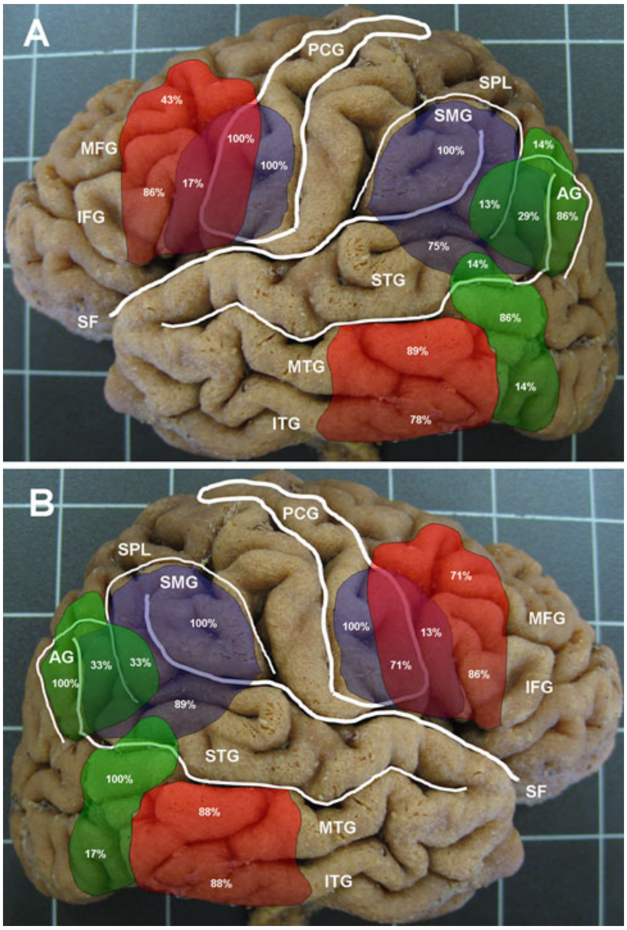

Fig. 8 Schematic representation of the cortical terminations of the three segments of the perisylvian superior longitudinal fasciculus (SLF) in the 18 hemispheres studied. A left hemisphere **(a)** and a right hemisphere **(b)** are represented. The cortical areas marked in *blue* represent the connections of the anterior segment of the SLF, connecting the supramarginal gyrus and the superior temporal gyrus with the precentral gyrus. The cortical areas marked in *green* represent the connections of the posterior segment of the SLF, connecting the posterior portion of the middle temporal gyrus with the angular gyrus. The cortical areas marked in *red* represent the connections of the arcuate fasciculus, connecting the middle and inferior temporal gyri, with the precentral gyrus and posterior portion of the inferior and middle frontal gyri. The percentages of tracts with connections to each lobule in the 18 hemispheres are presented. *AG* angular gyrus; *IFG* inferior frontal gyrus; *ITG* inferior temporal gyrus; *MFG* middle frontal gyrus; *PCG* precentral gyrus; *SF* sylvian fissure; *SMG* supramarginal gyrus; *SPL* superior parietal lobe; *STG* superior temporal gyrus

components of the perisylvian SLF. It is worth mentioning that in Fernandez-Miranda's paper, the cortex and superficial white matter were removed to reveal the anterior portion of the perisylvian SLF. This extensive removal of surrounding brain tissue eliminates important cortical landmarks making it impossible to analyze the precise cortical terminations of a specific fiber tract. Consequently, their dissection figures reveal horizontally oriented fibers located in the frontal and parietal operculum, but not the fibers projecting into the cortex ((Fernandez-Miranda et al. 2008b) Fig. 3a, c, d, p. 969). In the present work, cortex-sparing fiber dissection enables us to isolate the entire fascicle with the fibers projecting into the cortex. Therefore, our work seems to be the first one in the literature to completely isolate by fiber dissection the anterior segment of the SLF.

Regarding the caudal connection of this tract, Catani et al. (2005) described that it terminates at the inferior parietal lobe. However, a closer look to their images reveals that the fibers of this bundle are projected into the anterior part of the inferior parietal lobe, i.e., to the supramarginal gyrus ((Catani et al. 2005) Figs. 3, 4, p. 11 and 12). Thiebaut de Schotten et al. (2011) recently analyzed with spherical deconvolution tractography and fiber dissection the anatomy of the fronto-parietal connections of the SLF. This tractography methodology models the diffusion signal as a distribution of multiple fiber orientations, enabling the reconstruction of the white matter tracts in voxels with crossing, kissing or fanning fibers (Dell'acqua et al. 2010). They described the SLF III as a perisylvian component of the SLF situated in the white matter of the parietal and frontal opercula and connecting the supramarginal gyrus with the ventral premotor and prefrontal regions. Makris et al. (2005) analyzed the anatomy of the SLF by means of DTI in four subjects, and isolated the same tract running within the parieto-frontal operculum. Interestingly, Glasser and Rilling (2008) in another DTI study identified a connection of the posterior portion of the superior temporal gyrus to the frontal lobe, and considered these fibers as part of the AF. In the present work, fiber dissection revealed that this tract was caudally connected to the supramarginal gyrus and to the posterior part of the superior temporal gyrus (in the region just posterior to the Heschl's gyrus). The study of brain surface anatomy reveals that the superior temporal gyrus continues with the supramarginal gyrus at the caudal end of the sylvian fissure (Rhoton 2002); therefore, to precisely understand the termination of the bundle it is necessary to clarify the anatomical boundaries that define these two areas. The Atlas of the Cerebral Sulci of Ono et al. (1990) defines the boundary between these two regions at the angle between the terminal ascending ramus of the sylvian fissure and the posterior ramus of the sylvian fissure (Fig. 2). Our dissections revealed that the fibers from these two areas had the same orientation and converged into the same bundle within the parietal and frontal operculum (Fig. 2). Based on these results, we suggest that the fibers from the posterior part of the superior temporal gyrus are part of the anterior portion of the perisylvian SLF and not of the AF as suggested by Glasser and Rilling (2008).

At the frontal lobe, the anterior portion of the SLF was mainly connected to the ventral portion of the precentral gyrus (Figs. 3, 8). This is in agreement with previous DTI tractography studies (Kaplan et al. 2010; Croxson et al. 2005). The ventral portion of the precentral gyrus is divided into two parts: the anterior part is the seat of Brodmann's area 6 (ventral premotor cortex). The posterior part is Brodmann's area 4, corresponding to the somatotopic representation of the tongue, lips and pharynx. Both areas have been involved in the final steps of speech production (Ingham et al. 2004; Shuster and Lemieux 2005; Duffau et al. 2003a). Lesions to the dominant premotor cortex and to the supramarginal gyrus or underlying white matter in the left side have been associated with the gestural impairments observed in ideomotor and buccofacial apraxia (Schmahmann and Pandya 2006; De Renzi 1989; Kareken et al. 2003; Naeser et al. 1989). In addition, intraoperative electrical stimulation (IES) of this pathway in the left side has induced reproducible articulatory disorders (dysarthria or anarthria) with high reproducibility (Duffau et al. 2003b, 2008, Duffau 2011). Based on these observations, Duffau has designated this bundle as the dorsal phonological pathway and has suggested the hypothesis of an articulatory loop, with possible relationships with the verbal working memory network. This hypothesis is in accordance with Baddeley's model (Baddeley 2003), in which phonological processing is divided into a phonological store (involving the left supramarginal gyrus) and an articulatory rehearsal module (distributed rather over the left inferior frontal area). Accordingly with the so-called motor theories of language understanding, feedback is a necessary component of speech articulation (Liberman et al. 1967; Liberman and Mattingly 1985; Hickok and Poeppel 2004). These theories suggest that the same process that are involved in production also participate in the perception of speech. The anterior portion of the SLF, connecting to the cortex right next to the primary auditory area with the speech output areas at the frontal lobe, is a very suitable tract to explain the feedback of articulation. At the same time, the voice generated in the mouth is also heard in the primary auditory cortex, and the information may be rapidly sent to the posterior portion of the superior temporal gyrus and to the supramarginal gyrus. Finally, it may be sent to the precentral gyrus via the anterior portion of the SLF for a precise monitoring of speech articulation.

Posterior segment of the perisylvian component of the SLF

The present study reveals that this tract interconnects the posterior portion of the MTG with the AG (Figs. 4, 5, 8). This bundle has previously been described in DTI and fiber dissection studies (Catani and de Thiebaut 2008; Fernandez-Miranda et al. 2008b; Barrick et al. 2007; Lawes et al. 2008; Catani et al. 2005). Lawes et al. (2008) compared the anatomy of the tract by fiber dissection and DTI tractography. The authors described a tract connecting the posterior temporal lobe with the inferior parietal lobe and the middle occipital gyrus. Catani et al. (2005) and Fernandez-Miranda et al. (2008b) also described that this tract was connected to the inferior parietal lobe. However, the analysis of their rendering revealed projections to the posterior part of the inferior parietal lobe, i.e., with the angular gyrus. Consequently, our dissections revealed a finding not reported to date, a clear segregation of connections within the inferior parietal lobe with the anterior portion of the perisylvian SLF connected to the supramarginal gyrus, and the posterior portion of the perisylvian SLF projecting into the angular gyrus. This anatomical segregation of the SLF fibers suggests a rostro-caudal organization of function within the dominant inferior parietal lobe: the supramarginal gyrus connected to the anterior component of the SLF implicated in articulation of speech (Schmahmann and Pandya 2006; De Renzi 1989; Kareken et al. 2003; Naeser et al. 1989; Duffau et al. 2003b), and the angular gyrus connected to the posterior component of the SLF implicated in language perception, namely in syllable discrimination and identification and in other tasks that require explicit attention to segmental information (Parker et al. 2005).

Long segment of the SLF or arcuate fasciculus

In agreement with previous DTI studies, we found a long direct connection between the temporal and frontal lobes representing the classical AF (Figs. 6, 7). Glasser and Rilling (2008) recently analyzed with DTI tractography the anatomy of the SLF in 20 hemispheres. In this study, an important leftward asymmetry in the anatomy of the AF was reported, as this connection was identified in all the left hemispheres, whereas in only 11 right hemispheres (55%). Other DTI studies have also identified a dominance of this fascicle to the left hemisphere (Nucifora et al. 2005; Parker et al. 2005; Powell et al. 2006; Catani et al. 2007). These results contrast with those obtained in our study, as the AF was identified in eight out of nine right hemispheres (89%) and in all left hemispheres and these differences were statistically not significant ($p > 0.05$). As discussed by Glasser and Rilling (2008), it is likely that these pathways are actually present, and the absence of the tracts may be explained by the sensitivity of the probabilistic crossing fiber algorithm of DTI reconstructions. If the sensitivity is increased, the probability of identifying the bundles is also higher.

Traditionally, the rostral terminus of the AF has been assigned to the pars opercularis and triangularis of the frontal lobe, i.e., the Broca's area. This was first stated by

Wernicke in 1874 and has been usually maintained to date (Aminoff et al. 2005; Obler and Gjerlow 1999; Ludwig and Klingler 1956; Makris et al. 2005; Nieuwenhuys et al. 1988). However, this classical view has recently been challenged by numerous DTI tractography studies. Bernal and Altman (2010) studied the connectivity of the AF in 12 normal right-handed subjects. A sagittal fractional anisotropy image was used to determine the rostral end point of the AF fibers in the white matter pertaining to specific gyri or pars of the frontal lobe. The authors identified strong connections of the AF to the precentral gyrus and minimal connections to the posterior portion of the inferior frontal gyrus in only 41.6% of the subjects. The general conclusion in this study is that the AF is not connected to the Broca's area, but instead mainly to the inferior portion of the precentral gyrus (ventral premotor cortex and primary motor area). Barrick et al. (2007), in a DTI study, also describe that at the frontal lobe most of the fibers of the AF turn sharply toward the precentral gyrus and only a small portion of the fibers continues to the pars opercularis of the IFG. However, these findings conflict with other recent reports of the arcuate connectivity with DTI tractography. Catani et al. (2005), Catani and de Thiebaut (2008) describe connections of the AF to the posterior part of the inferior and middle frontal gyrus and to the precentral gyrus. These findings are in agreement with those of Glasser and Rilling (2008) that identified projections of the AF into the posterior portion of the middle frontal gyrus, dorsal portion of the precentral gyrus and to the middle and posterior portions of the inferior frontal gyrus. At the level of the frontal operculum, the fibers of the AF intersect the terminal branches of the anterior portion of the SLF and the inferior fronto-occipital fasciculus. DTI tractography is inaccurate to map the fiber architecture in areas where the trajectories of different fibers intersect (Catani et al. 2005); consequently, the strong intersection of fibers at the frontal operculum may explain the controversy in DTI studies regarding the frontal termination of the AF. In the present study, due to strong intersections of fibers at the level of the frontal operculum, it was not possible to follow the terminal fibers in three hemispheres. However, in the rest of the hemispheres, strong connections of the AF to the precentral gyrus were identified, and, as shown in Fig. 3, we also isolated fibers that projected into the posterior portion of the inferior and middle frontal gyrus. Catani et al. (2005) named this extended region Broca's territory, as it included in addition to the classical Broca's area other cortical regions specialized in higher level aspects of language.

Important controversy also exists in the literature regarding the temporal projection of the AF. Some authors consider that it projects to a very specific region located at the posterosuperior temporal sulcus and gyrus, i.e., the classical Wernicke area (Glasser and Rilling 2008). These findings apparently conflict with those obtained by Glasser and Rilling (2008) and by Catani et al. (2005), Bernal and Ardila (2009) and Barrick et al. (2007). These authors consider that the AF projects into an extended area rather than a localized center, including the posterior part of both the superior and middle temporal gyri. Other authors describe projections into a wider area of the temporal lobe, including the medial and posterior portions of the superior, middle and inferior temporal gyri (Turken and Dronkers 2011). Our dissections also revealed important connections of the AF with the middle and inferior temporal gyri (Figs. 6, 8). Connections of the AF to the anterior portion of the superior temporal gyrus were not identified; this may be explained by the strong intersection with the fibers of the acoustic radiations (terminating at the Heschl's gyrus).

Therefore, the present work showed a particularly rich connectivity profile of the middle temporal gyrus, as it is connected to both the anterior portion of the SLF and AF. Turken and Dronkers (2011) had previously reported this high connectivity of the middle temporal gyrus, evidencing that it is also connected to the inferior fronto-occipital fasciculus, middle longitudinal fasciculus, inferior longitudinal fasciculus and posterior corpus callosum fibers. Based on the high connectivity of this area and the severity of the impairments associated with middle temporal gyrus lesions, it has been suggested that this region holds a key position in language comprehension. Mesulam introduced the concept of large-scale functional networks; based on this model of neural processing, cognitive functions are the result of a collaborative interaction of multiple interconnected networks that are widely distributed within the brain (Mesulam 1990, 2009). These networks also include core regions that serve as transmodal gateways; lesions affecting such gateways would produce multiple disconnections, disrupting upstream and downstream network functions. Based on the high connectivity of the middle temporal gyrus, it has been suggested that this area represents such a critical neural epicenter within the perisylvian language network (Price 2000; Hickok and Poeppel 2004). In fact, this region is strategically located on the boundary between auditory and visual association cortex, receiving inputs from both the primary auditory cortex, as well as extrastriate visual cortex (Dronkers et al. 2004; Turken and Dronkers 2011). All these observations give a plausible explanation for the severe and persisting language comprehension impairments that follow a lesion to the middle temporal gyrus and underlying white matter (Duffau et al. 2002; Leclercq et al. 2010).

In addition to the sequelae related to a cortical injury, a lesion specifically disrupting the AF will cause a disconnection between the posterior temporal and frontal lobes. IES of a white matter tract induces a virtual transitory disconnection giving a unique opportunity to study the function of this network. IES of the AF has induced reproducible phonemic paraphasias, namely disorders that affect the phonological form of the words. The target word is transformed by substitution, elision, addition or transposition of one or more phonemes (Saur et al. 2008; Duffau et al. 2002; Leclercq et al. 2010). Based on these observations, and an accumulation of knowledge coming from neuroimaging, neuropsychology and psycholinguistic, the AF has been proposed as the dorsal phonological route for language function (Hickok and Poeppel 2004), in accordance with the dual-stream model that segregates phonological and semantic processing (Young 1997; Naeser et al. 1982). Unlike a transitory dysfunction, a structural lesion to the AF in the left hemisphere has been associated with conductive aphasia, characterized by repetition impairment and phonemic paraphasias (Schmahmann et al. 2007). This tract is frequently damaged by small infarcts or other insults at the level of the white matter underling the inferior parietal lobe. The present work revealed that the distance between the caudal end of the insula and the posterior edge of the AF ranged between 11 and 25 mm; we also observed that the AF underlies the caudal end of the inferior parietal lobe (the angular gyrus). This small white matter region is a vulnerable part of the network when neurological damage occurs, as multiple fibers from the temporal cortex converge within this area. Consequently, a small lesion in this strategic place may have more serious consequences than a comparable lesion elsewhere in the network. These data are paramount for neurosurgical approaches to lesions deep into the inferior parietal lobe; in addition to the cortical lesion at the level of the supramarginal or angular gyrus, the pathway may be damaged in the underling white matter. Consequently, the neurosurgeon should find an alternative route to access these lesions or use intraoperative electrical stimulation to avoid damage to the tract (Maldonado et al. 2011).

Study limitations:

Our findings in this study are subject to some limitations

- Fiber dissection has a limited value to study white matter connectivity in areas of crossing fibers. At the level of the frontal operculum, the fibers of the SLF strongly intersect with the terminal branches of other long association fasciculus (especially to the inferior fronto-occipital fasciculus). In the present study in 3 of the 12 hemispheres dissected, it was not possible to follow the frontal termination of the AF and anterior portion of the SLF. On the other hand, dissection enabled the isolation of fibers up to 2 mm in diameter. Consequently, with this technique it was not possible to follow smaller branches of the SLF.
- Even though DTI tractography has extensively been used to study white matter connectivity, it has three inherent shortcomings: (1) first, same as in fiber dissection, is the inaccuracy of this technique to map the fiber architecture in areas where the trajectories of different fibers intersect (Wang et al. 2008). Several diffusion imaging techniques have been developed to reduce the fiber intersecting problem. Some of these MR-based approaches "beyond the diffusion tensor" are called diffusion spectrum imaging (Wedeen et al. 2005), q-ball imaging (Tuch et al. 2003) and spherical deconvolution (Dell'acqua et al. 2010; Thiebaut de Schotten et al. 2011). (2) Second is the difficulties in distinguishing the different fascicles in areas where tracts run in parallel (e.g., the optic radiations and the fibers of the IFOF) (Catani et al. 2003). (3) Third is the inability to follow the terminal branches of the white matter bundles: it is only possible to infer their final cortical destinations from the location and orientation of the average tract end points (Tomasi and Volkow 2011). Novel approaches to solve this problem have been proposed, such as tract reconstruction based on their anatomical termination near the gray–white matter boundary (Lawes et al. 2008) and a postmortem neuroimaging technique called 3D polarized light imaging (Axer et al. 2011). In addition, high-field MRI of postmortem brains already demonstrated its potential to reveal cortical connections more reliably (Soria et al. 2011).
- Although all subjects were adults, there was a wide age difference between subjects studied with fiber dissection (mean 69 years) and those studied with DTI tractography (mean 28 years). This may have affected the data, as white matter connectivity may change with age. However, the major observations of this work were consistent across the majority of subjects studied with DTI tractography and fiber dissection.

Conclusions

In the present work, fiber dissection of postmortem human brains and DTI tractography enabled the isolation of the three components of the perisylvian SLF. With the technique of cortex-sparing fiber dissection, the cortex and superficial white matter were preserved along the dissection, enabling the isolation of the fibers projecting into the cortex and to analyze the exact cortical terminations of each of the subcomponents of the SLF. The following portions and cortical connections were identified: (1) anterior segment, connecting the supramarginal gyrus and superior temporal gyrus with the precentral gyrus;

(2) posterior segment, connecting the posterior portion of the middle temporal gyrus with the angular gyrus; and (3) the AF that connects the middle and inferior temporal gyri with the precentral gyrus and posterior portion of the inferior and middle frontal gyri.

The functional role of a tract may be inferred from its topography within the brain. The segregation of the perisylvian SLF into three components defined by DTI studies established the first step to understanding the function of this large-scale network. Based on these observations, it has been hypothesized that each component of this tract is specialized in transmitting different types of information. However, to elucidate how each part is functionally integrated within the overall network, it is necessary to accurately define the cortical connectivity. Each brain region acquires its particular function in a brain network by virtue of how it interacts with other regions. Consequently, based on the known functional role of these cortical areas, it is possible to develop new insights into the putative functional properties of these connections.

Acknowledgments Juan Martino received specific funding from the 11/18 API Grant entitled "Estudio de la conectividad conectividad cerebral mediante disección de fibras estructural", "Fundación Marqués de Valdecilla", IFIMAV, Santander, Cantabria, Spain, 8 October 2010.

References

Aminoff MJ, Greenberg DA, Simon RP (2005) Clinical neurology. McGraw-Hill, New York

Axer H, Beck S, Axer M, Schuchardt F, Heepe J, Flucken A, Axer M, Prescher A, Witte OW (2011) Microstructural analysis of human white matter architecture using polarized light imaging: views from neuroanatomy. Front Neuroinform 5:28

Baddeley A (2003) Working memory: looking back and looking forward. Nat Rev Neurosci 4:829–839

Barrick TR, Lawes IN, Mackay CE, Clark CA (2007) White matter pathway asymmetry underlies functional lateralization. Cereb Cortex 17:591–598

Bernal B, Altman N (2010) The connectivity of the superior longitudinal fasciculus: a tractography DTI study. Magn Reson Imaging 28:217–225

Bernal B, Ardila A (2009) The role of the arcuate fasciculus in conduction aphasia. Brain 132:2309–2316

Catani M, de Thiebaut SM (2008) A diffusion tensor imaging tractography atlas for virtual in vivo dissections. Cortex 44:1105–1132

Catani M, Howard RJ, Pajevic S, Jones DK (2002) Virtual in vivo interactive dissection of white matter fasciculi in the human brain. Neuroimage 17:77–94

Catani M, Jones DK, Donato R, Ffytche DH (2003) Occipito-temporal connections in the human brain. Brain 129:2093–2107

Catani M, Jones DK, Ffytche DH (2005) Perisylvian language networks of the human brain. Ann Neurol 57:8–16

Catani M, Allin MP, Husain M, Pugliese L, Mesulam MM, Murray RM, Jones DK (2007) Symmetries in human brain language pathways correlate with verbal recall. Proc Natl Acad Sci USA 104:17163–17168

Choi C, Rubino PA, Fernandez-Miranda JC, Abe H, Rhoton AL Jr (2006) Meyer's loop and the optic radiations in the transylvian approach to the mediobasal temporal lobe. Neurosurgery 59:ONS228–ONS235

Croxson PL, Johansen-Berg H, Behrens TE, Robson MD, Pinsk MA, Gross CG, Richter W, Richter MC, Kastner S, Rushworth MF (2005) Quantitative investigation of connections of the prefrontal cortex in the human and macaque using probabilistic diffusion tractography. J Neurosci 25:8854–8866

De Renzi E (1989) Agnosia. Recenti Prog Med 80:633–637

Dell'acqua F, Scifo P, Rizzo G, Catani M, Simmons A, Scotti G, Fazio F (2010) A modified damped Richardson-Lucy algorithm to reduce isotropic background effects in spherical deconvolution. Neuroimage 49:1446–1458

Dronkers NF, Wilkins DP, Van VR Jr, Redfern BB, Jaeger JJ (2004) Lesion analysis of the brain areas involved in language comprehension. Cognition 92:145–177

Duffau H (2011) The "frontal syndrome" revisited: lessons from electrostimulation mapping studies. Cortex (Epub ahead of print)

Duffau H, Capelle L, Sichez N, Denvil D, Lopes M, Sichez JP, Bitar A, Fohanno D (2002) Intraoperative mapping of the subcortical language pathways using direct stimulations. An anatomo-functional study. Brain 125:199–214

Duffau H, Capelle L, Denvil D, Gatignol P, Sichez N, Lopes M, Sichez JP, Van ER (2003a) The role of dominant premotor cortex in language: a study using intraoperative functional mapping in awake patients. Neuroimage 20:1903–1914

Duffau H, Gatignol P, Denvil D, Lopes M, Capelle L (2003b) The articulatory loop: study of the subcortical connectivity by electrostimulation. Neuroreport 14:2005–2008

Duffau H, Gatignol P, Mandonnet E, Capelle L, Taillandier L (2008) Intraoperative subcortical stimulation mapping of language pathways in a consecutive series of 115 patients with Grade II glioma in the left dominant hemisphere. J Neurosurg 109: 461–471

Fernandez-Miranda JC, Rhoton AL Jr, Kakizawa Y, Choi C, varez-Linera J (2008a) The claustrum and its projection system in the human brain: a microsurgical and tractographic anatomical study. J Neurosurg 108:764–774

Fernandez-Miranda JC, Rhoton AL Jr, varez-Linera J, Kakizawa Y, Choi C, de Oliveira EP (2008b) Three-dimensional microsurgical and tractographic anatomy of the white matter of the human brain. Neurosurgery 62:989–1026

Gharabaghi A, Kunath F, Erb M, Saur R, Heckl S, Tatagiba M, Grodd W, Karnath HO (2009) Perisylvian white matter connectivity in the human right hemisphere. BMC Neurosci 10:15

Giolli RA, Gregory KM, Suzuki DA, Blanks RH, Lui F, Betelak KF (2001) Cortical and subcortical afferents to the nucleus reticularis tegmenti pontis and basal pontine nuclei in the macaque monkey. Vis Neurosci 18:725–740

Glasser MF, Rilling JK (2008) DTI tractography of the human brain's language pathways. Cereb Cortex 18:2471–2482

Hagmann P, Thiran JP, Jonasson L, Vandergheynst P, Clarke S, Maeder P, Meuli R (2003) DTI mapping of human brain connectivity: statistical fibre tracking and virtual dissection. Neuroimage 19:545–554

Henry RG, Berman JI, Nagarajan SS, Mukherjee P, Berger MS (2004) Subcortical pathways serving cortical language sites: initial experience with diffusion tensor imaging fiber tracking combined with intraoperative language mapping. Neuroimage 21:616–622

Hickok G, Poeppel D (2004) Dorsal and ventral streams: a framework for understanding aspects of the functional anatomy of language. Cognition 92:67–99

Ingham RJ, Fox PT, Ingham JC, Xiong J, Zamarripa F, Hardies LJ, Lancaster JL (2004) Brain correlates of stuttering and syllable production: gender comparison and replication. J Speech Lang Hear Res 47:321–341

Kaplan E, Naeser MA, Martin PI, Ho M, Wang Y, Baker E, Pascual-Leone A (2010) Horizontal portion of arcuate fasciculus fibers track to pars opercularis, not pars triangularis, in right and left hemispheres: a DTI study. Neuroimage 52:436–444

Kareken DA, Mosnik DM, Doty RL, Dzemidzic M, Hutchins GD (2003) Functional anatomy of human odor sensation, discrimination, and identification in health and aging. Neuropsychology 17:482–495

Kier EL, Staib LH, Davis LM, Bronen RA (2004a) Anatomic dissection tractography: a new method for precise MR localization of white matter tracts. AJNR Am J Neuroradiol 25:670–676

Kier EL, Staib LH, Davis LM, Bronen RA (2004b) MR imaging of the temporal stem: anatomic dissection tractography of the uncinate fasciculus, inferior occipitofrontal fasciculus, and Meyer's loop of the optic radiation. AJNR Am J Neuroradiol 25:677–691

Klingler J (1935) Erleichterung der makroskopischen Praeparation des Gehirns durch den Gefrierprozess. Schweiz Arch Neurol Psychiatr 36:247–256

Klingler J, Gloor P (1960) The connections of the amygdala and of the anterior temporal cortex in the human brain. J Comp Neurol 115:333–369

Lawes IN, Barrick TR, Murugam AB, Spierings N, Evans DR, Song M, Clarke CA (2008) Atlas-based segmentation of white matter tracts of the human brain using diffusion tensor tractography and comparison with classical dissection. Neuroimage 39:79

Le BD, Mangin JF, Poupon C, Clark CA, Pappata S, Molko N, Chabriat H (2001) Diffusion tensor imaging: concepts and applications. J Magn Reson Imaging 13:534–546

Leclercq D, Duffau H, Delmaire C, Capelle L, Gatignol P, Ducros M, Chiras J, Lehericy S (2010) Comparison of diffusion tensor imaging tractography of language tracts and intraoperative subcortical stimulations. J Neurosurg 112:503–511

Liberman AM, Mattingly IG (1985) The motor theory of speech perception revised. Cognition 21:1–36

Liberman AM, Cooper FS, Shankweiler DP, Studdert-Kennedy M (1967) Perception of the speech code. Psychol Rev 74:431–461

Ludwig E, Klingler J (1956) Atlas Cerebri Humani: Der innere Bau des Gehirns dargestellt auf Grund mackroskopischer Präparate. Brown, Boston

Makris N, Kennedy DN, McInerney S, Sorensen AG, Wang R, Caviness VS Jr, Pandya DN (2005) Segmentation of subcomponents within the superior longitudinal fascicle in humans: a quantitative, in vivo DT-MRI study. Cereb Cortex 15:854–869

Maldonado IL, Moritz-Gasser S, Duffau H (2011) Does the left superior longitudinal fascicle subserve language semantics? A brain electrostimulation study. Brain Struct Funct (In press)

Martino J, Brogna C, Robles SG, Vergani F, Duffau H (2010a) Anatomic dissection of the inferior fronto-occipital fasciculus revisited in the lights of brain stimulation data. Cortex 46: 691–699

Martino J, Vergani F, Robles SG, Duffau H (2010b) New insights into the anatomic dissection of the temporal stem with special emphasis on the inferior fronto-occipital fasciculus: implications in surgical approach to left mesiotemporal and temporoinsular structures. Neurosurgery 66:4–12

Martino J, De Witt Hamer PC, Vergani F, Brogna C, de Lucas EM, Vazquez-Barquero A, Garcia-Porrero JA, Duffau H (2011) Cortex-sparing fiber dissection: an improved method for the study of white matter anatomy in the human brain. J Anat 219:531–541. doi:10.1111/j.1469-7580.2011.01414.x (Epub ahead of print)

Mesulam MM (1990) Large-scale neurocognitive networks and distributed processing for attention, language, and memory. Ann Neurol 28:597–613

Mesulam M (2009) Defining neurocognitive networks in the BOLD new world of computed connectivity. Neuron 62:1–3

Mori S, van Zijl PC (2002) Fiber tracking: principles and strategies: a technical review. NMR Biomed 15:468–480

Naeser MA, Alexander MP, Helm-Estabrooks N, Levine HL, Laughlin SA, Geschwind N (1982) Aphasia with predominantly subcortical lesion sites: description of three capsular/putaminal aphasia syndromes. Arch Neurol 39:2–14

Naeser MA, Palumbo CL, Helm-Estabrooks N, Stiassny-Eder D, Albert ML (1989) Severe nonfluency in aphasia. Role of the medial subcallosal fasciculus and other white matter pathways in recovery of spontaneous speech. Brain 112(Pt 1):1–38

Nieuwenhuys R, Voogd J, van Huijzen C (1988) The human central nervous system. Springler-Verlag, Berlin

Nucifora PG, Ragini Verma CA, Melhem ER, Gur RE, Gur RC (2005) Lefward asymmetry in relative fiber density of the arcuate fasciculus. Neuroreport 16:791–794

Obler LK, Gjerlow K (1999) Language and the brain. Cambridge University Press, Cambridge

Ono M, Kubik S, Abernathey CD (1990) Atlas of the cerebral sulci. Georg Thieme Verlag, New York

Parker GJ, Luzzi S, Alexander DC, Wheeler-Kingshott CA, Ciccarelli O, Lambon Ralph MA (2005) Lateralization of ventral and dorsal auditory-language pathways in the human brain. Neuroimage 24:656–666

Petrides M, Pandya DN (1984) Projections to the frontal cortex from the posterior parietal region in the rhesus monkey. J Comp Neurol 228:105–116

Petrides M, Pandya DN (2009) Distinct parietal and temporal pathways to the homologues of Broca's area in the monkey. PLoS Biol 7:e1000170

Peuskens D, van Loon J, Van Calenbergh F, van den Bergh R, Goffin J, Plets C (2004) Anatomy of the anterior temporal lobe and the frontotemporal region demonstrated by fiber dissection. Neurosurgery 55:1174–1184

Powell HW, Parker GJ, Alexander DC, Symms MR, Boulby PA, Wheeler-Kingshott CA, Barker GJ, Noppeney U, Koepp MJ, Duncan JS (2006) Hemispheric asymmetries in language-related pathways: a combined functional MRI and tractography study. Neuroimage 32:388–399

Price CJ (2000) The anatomy of language: contributions from functional neuroimaging. J Anat 197:335–359

Rhoton AL Jr (2002) The cerebrum. Neurosurgery 51:S1–S51

Rilling JK, Glasser MF, Preuss TM, Ma X, Zhao T, Hu X, Behrens TE (2008) The evolution of the arcuate fasciculus revealed with comparative DTI. Nat Neurosci 11:426–428

Saur D, Kreher BW, Schnell S, Kummerer D, Kellmeyer P, Vry MS, Umarova R, Musso M, Glauche V, Abel S, Huber W, Rijntjes M, Hennig J, Weiller C (2008) Ventral and dorsal pathways for language. Proc Natl Acad Sci USA 105:18035–18040

Schmahmann JD, Pandya DN (2006) Fiber pathways of the brain. Oxford UP, New York

Schmahmann JD, Rosene DL, Pandya DN (2004) Motor projections to the basis pontis in rhesus monkey. J Comp Neurol 478: 248–268

Schmahmann JD, Pandya DN, Wang R, Dai G, D'Arceuil HE, de Crespigny AJ, Wedeen VJ (2007) Association fibre pathways of the brain: parallel observations from diffusion spectrum imaging and autoradiography. Brain 130:630–653

Shuster LI, Lemieux SK (2005) An fMRI investigation of covertly and overtly produced mono- and multisyllabic words. Brain Lang 93:20–31

Sincoff EH, Tan Y, Abdulrauf SI (2004) White matter fiber dissection of the optic radiations of the temporal lobe and implications for surgical approaches to the temporal horn. J Neurosurg 101: 739–746

Soria G, De NM, Tudela R, Blasco G, Puig J, Planas AM, Pedraza S, Prats-Galino A (2011) Improved assessment of ex vivo brainstem neuroanatomy with high-resolution MRI and DTI at 7 Tesla. Anat Rec (Hoboken.) 294:1035–1044

Thiebaut de Schotten M, Dell'acqua F, Forkel SJ, Simmons A, Vergani F, Murphy DG, Catani M (2011) A lateralized brain network for visuospatial attention. Nat Neurosci 14:1245–1246

Tomasi D, Volkow ND (2011) Aging and functional brain networks. Mol Psychiatry Jul 5. doi:10.1038/mp.2011.81

Tuch DS, Reese TG, Wiegell MR, Wedeen VJ (2003) Diffusion MRI of complex neural architecture. Neuron 40:885–895

Ture U, Yasargil MG, Pait TG (1997) Is there a superior occipito-frontal fasciculus? A microsurgical anatomic study. Neurosurgery 40:1226–1232

Ture U, Yasargil DC, Al-Mefty O, Yasargil MG (1999) Topographic anatomy of the insular region. J Neurosurg 90:720–733

Ture U, Yasargil MG, Friedman AH, Al-Mefty O (2000) Fiber dissection technique: lateral aspect of the brain. Neurosurgery 47:417–426

Turken AU, Dronkers NF (2011) The neural architecture of the language comprehension network: converging evidence from lesion and connectivity analyses. Front Syst Neurosci 5:1

Wang F, Sun T, Li X-G, Liu N-J (2008) Diffusion tensor tractography of the temporal stem on the inferior limiting sulcus. J Neurosurg 108:775–781

Wedeen VJ, Hagmann P, Tseng WY, Reese TG, Weisskoff RM (2005) Mapping complex tissue architecture with diffusion spectrum magnetic resonance imaging. Magn Reson Med 54:1377–1386

Young P (1997) Basic Clinical Neuroanatomy. Williams and Wilkins, Philadelphia